Net thrust measurement of propellantless microwave thrusters*

Yang Juan** Wang Yuquan Li Pengfei Wang Yang Wang Yunmin Ma Yanjie

(Northwestern Polytechnical University, College of Aeronautics, Xi'an 710072) (Received June 9, 2011; revised manuscript received in October 25, 2011)

According to classical electromagnetic theory, this paper introduces a new kind of propellantless microwave thruster device for use in space propulsion. This device is able to directly convert microwave radiation into thrust without the need for any propulsion medium. The difference with traditional space propulsion devices is that this system means there is no need to carry a large propellant tank, and the problems of plume emissions polluting the space craft can be eliminated. The system comprises a frustum microwave resonator, microwave source, and load. The microwave source produces microwave radiation which can be input into the frustum microwave resonator and form a pure standing wave and electromagnetic pressure gradient. Thus, along the axial direction of the frustum microwave resonator, net thrust is formed. This article, based on the indifferent equilibrium principle, overcomes the weight and rigidity resistance of the thruster itself, and successfully measures the net thrust produced by the propellantless microwave thruster. The results show that: Based on classical electromagnetic theory, creating a propellantless microwave propulsion system can produce a net thrust; when the microwave source output is 2.45GHz, with a microwave power of 80-2500W, the propulsion produced by the thruster is located in the range of 70-720mN, and the total measurement error is less than 12%.

Key words: Electromagnetic wave theory, Maxwell stress tensor, Electromagnetic processes and characteristics PACS: 03.50. De, 41. 20. Jb, 13. 40. –f

* National Natural Sciences Foundation (Approval Number: 90716019) Assisted

** E-mail: yangjuan@nwpu.edu.cn

1 Introduction

Traditional plasma propulsion device systems such as Hall thrusters, ion thrusters and arc thrusters are currently the space propulsion devices which are most applied in domestic and foreign research. Compared to chemical space propulsion devices, they have rather high specific impulse and long life characteristics. These propulsion devices can be used as power systems for satellite attitude control and location control, and in deep space main propulsion systems [1-10]. In space missions, traditional plasma body propulsion devices must ionize a large amount of working medium into a plasma body. Then some kind of acceleration mechanism is used to enable the high speed ions to produce thrust. These kinds of mechanism solve the existing problem of plasma propulsion device plumes interfering with spacecraft. Solar sail propulsion is a kind of propellantless propulsion device. As long as the solar sail can collect enough solar radiation, it can drive the spacecraft forward [11]. The solar sail propulsion concept was raised 100 years ago, but with the emergence of microelectronics and thin membrane materials technology, modern day researchers have started

theoretical and experimental studies of solar sails. In 2010, Japan launched a spacecraft called IKAROS, this was the first historical confirmation of the feasibility of solar sail propulsion for spacecraft [12]. Microwave sails are similar to solar sails. They are another kind of propellantless propulsion device. This device uses a huge concave thin metal membrane as the microwave sail. During space travel, surface microwave radiation source energy flow can cause the craft to continually move forward. Compared to a traditional plasma body propulsion device, solar sails and microwave sails are able to work properly without work medium. Thus, the spacecraft can be given better mobility, the necessity for carrying huge work medium stores can be avoided, and the problem of spacecraft plume interfering with the spacecraft surface is resolved.

As shown in Figure 1, we designed and developed another propellantless propulsion device - a propellantless microwave thruster system. The system comprises an integrated microwave source, circulator, waveguide, the frustum microwave resonator and load. From which the frustum microwave resonator is also the thruster cavity. This is the key component for thrust. The difference from solar sails and microwave sails is that this system does not take advantage of the radiation in empty space to produce thrust; rather it uses the electromagnetic pressure gradient acting on the frustum microwave resonator to produce net thrust. This mode of operation has a simple and compact structure, high efficiency and easily controllable thrust.

Roger Shawyer of British Satellite Propulsion Research Co., Ltd. (SPR Ltd.) conducted important research into propellantless microwave thrusters. Roger Shawyer called the propellantless microwave propulsion devices the "electromagnetic drive" (emdrive). In 2003, he developed the first emdrive. Its diameter is 160mm, and its microwave power consumption is 850W. Using a balance beam method, the obtained actual thrust value was measured at 16mN. In 2006, Roger Shawyer developed a second emdrive. Its diameter is 280mm, and its power consumption is 1200W. Using horizontal and hanging measurement programs to measure the thrust, the obtained actual thrust value was 250mN. In 2007, Roger Shawyer carried out dynamic testing in a low-resistance suspended rotating platform. The results of the experiment were that when the second emdrive consumed microwave power of 1000W, thrust reached 287mN and the 100kg air suspension platform was accelerated to 2cm / s.

Northwestern Polytechnical University began to study the propellantless microwave propulsion in 2008, using classical electromagnetic theory to explain the source of thrust used in propellantless microwave propulsion devices [14, 15]. The theoretical feasibility of the device was discussed. Northwestern Polytechnical University also proposed a frustum microwave resonator design method based on electromagnetic value simulation analysis and experimentally tuned propellantless microwave propulsion. At the same time, the University designed and developed the first set of propellantless microwave propulsion devices in China.

Although the British carried out pioneering research work on the emdrive, the thrust measurement programs lack scientific descriptions. Furthermore, to date, the research paper has not been published in official journals. In China, scientific research was carried out from a theoretical and experimental basis on propellantless microwave propulsion devices. However, propellantless microwave thruster device net thrust measurement results have not been scientifically provided from an experimental perspective. This paper uses a nationally patented device - the rocket indifferent equilibrium thrust measurement device - to measure the propellantless microwave

thruster net thrust. Thus further experimentally verifying the feasibility of the practical microwave propulsion device.

2 The principle and thrust measurement system of propellantless microwave thrusters

2.1 The principle of propellantless microwave thrusters

In the system shown in Figure 1, the microwave source transfers electrical energy into microwave energy and along the waveguide and circulator is transmitted to the frustum microwave resonator. When the frustum microwave resonator's fixed resonant frequency and microwave output electromagnetic wave frequency are identical, the electromagnetic frustum microwave resonator resonant frequency forms an electromagnetic pressure gradient along the direction of the cavity, resulting in a substantial net thrust. The frustum microwave resonator is a sealed cavity enclosed by metal. When wave resonance occurs inside the cavity, the following important features occur: When not considering other energy losses, the only microwave energy loss caused to the frustum microwave resonator occurs at cavity wall skin depth; the frustum microwave resonator has an amplification effect on the electric field and magnetic field power. However, it is not in violation of the conservation of energy. According to Maxwell's equations and electromagnetic wave energy flux density vectors, the overall electromagnetic field in the cavity will create electromagnetic pressure; if you select a suitable electromagnetic field distribution law, an electromagnetic pressure gradient is formed along the direction of the frustum microwave resonator. Dividing the electromagnetic pressure along the cavity surface into surface integrals, the thrust produced along the frustum microwave resonator axial direction can be obtained.

Frustum microwave resonator (thruster cavity)

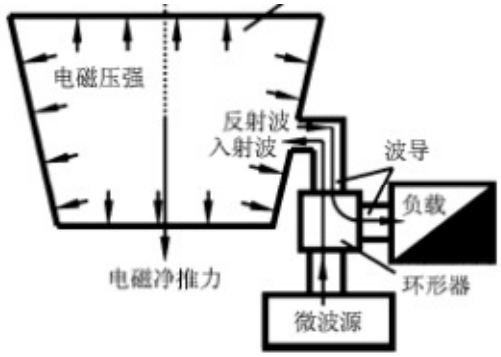

Figure 1 Propellantless microwave thruster device structural diagram

[Labels top to bottom: Electromagnetic pressure; reflected waves; entering waves; waveguide; load; circulator; electromagnetic net thrust; microwave source]

2.2 Thrust measurement system

As shown in Figure 2, the propellantless microwave thruster indifferent equilibrium thrust measurement device comprises an electrical circuit and thrust measurement rack. The thrust measurement rack comprises mobile and fixed components. The mobile component includes a frustum microwave resonator 1, horizontal beam 2, mobile left and right electromagnetic coils 3 and 4, angle displacement sensor and acceleration sensor mobile part 6, fixed on offset plate 5, support 7, counterweight 8, flexible waveguide 9 and standard scale 10. Using a knife tip structure on fulcrums O_1 and O_2, the mobile part is supported on the base. The fixing member is fixedly connected to the base; it includes the mobile left and right electromagnetic coils 3 and 4, angular displacement sensor and accelerator sensor fixed parts 11, and fixed frame 12. The circuit signal includes angular displacement sensor signal amplifier K_θ, and accelerator signal amplifier $K_{\theta\text{-}}$, compound amplifier K_Σ, sample resistance R and voltage display instrument V, from which mobile gravity line L_1, base fulcrum O_1 and O_2 form a straight line L_2 as a shaft. The entire mobile part can rotate L_2 rotations within a microscopic angle range. Based on the installation orientation of Figure 2, when the thruster is working normally, if the electromagnetic coil 3 is working, the net thrust is from the microwave resonator large end to the small end; if the electromagnetic coil 4 is working, the net thrust is from the microwave resonator small end to the large end.

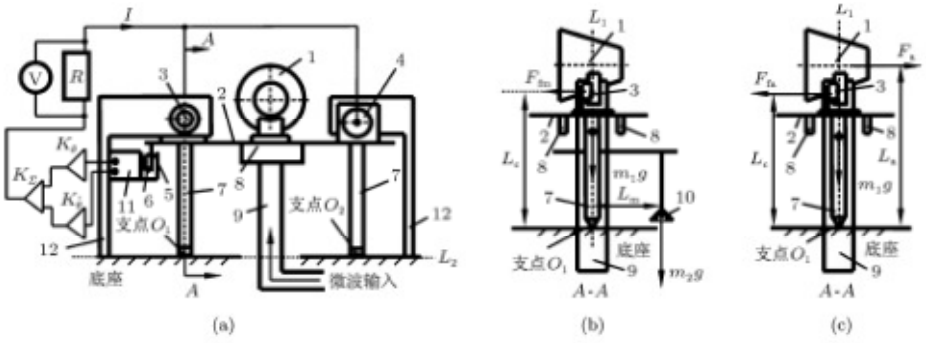

Figure 2 propellantless microwave thruster thrust measurement device structure (a) Main schematic; (b) Standard weight A-A sectional side view; (c) A-A sectional side view with the thruster under net thrust

[Labels left to right, top to bottom (a): Fulcrum O_1, Fulcrum O_2, Base, Microwave input; (b) Fulcrum O_1, base; (c): Fulcrum O_1, base]

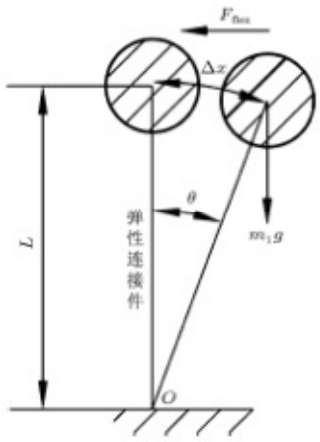

Figure 3 elastic and gravity schematics

[Label: Elastic connecting part]

Figure 2 shows the thrust measurement device accurately measuring the thrust with the following standard steps.

1) Adjustment of the balance inside the device, eliminating the system's internal rigidity and weight impacting on the thrust measurement. Under the weight of moving parts, flexible waveguide 9 will produce an elastic force Fflex. If the mass of the system is concentrated to a small ball, the flexible waveguide is equivalent to the conventional elastic connecting part, and the elastic force and weight balance diagram is as shown in Figure 3. Before the propellantless microwave thrusters work, the rigidity of flexible waveguide 9, and mass and position of counterweight 8 must be adjusted, so that the flexible waveguide moment of elastic force FflexL balances the gravitational moment of the mobile parts $m_1 g\Delta x$. At the same time, the mobile part's line of gravity L_1 and rotational axis L_2 intersect. At this time the rigidity and weight of the system components can be eliminated from the thrust measurement.

2) Balance adjustments for the thrust measurement device under external force, so that the measured force moment and electromagnetic coil moment balance. When the moving parts are under external force, they will make micro-angle rotations around rotation axis L_2. At this time, the angular displacement and acceleration sensor mobile parts 6 will trigger the circuit to form a feedback current L which will feedback into the electromagnetic coil 3 and 4 and then produce a feedback electromagnetic moment FfaLc balancing the external force on the mobile parts; Ffa is the feedback electromagnetic force; Lc is the feedback electromagnetic force arm. At this time, the rotation of the mobile parts is then suppressed, and the thrust measurement device again reaches equilibrium.

3) Calibration of the thrust measuring device. When the mobile parts are only subject to the standard force of gravity of $10m_2 g$, the angular displacement and accelerator sensor mobile part 6 again triggers the circuit to form a feedback current, and the electromagnetic coil produces electromagnetic force Ffm. The set thruster net thrust arm La is double the standard gravity arm Lm. That is La = 2Lm. At the same time, strictly using the linear relationship of the design circuit system,

and suitably selecting the sampling resistance and voltage display meter range can cause the voltage to display exactly the half of the standard gravity and the same size as the thruster net thrust Fa. Therefore, for different standard weights, the readout voltage value can be calibrated for the thrust measurement device.

4) Thrust measurement device zero point processing. After completing the balance adjustments within the system, ideally, measurement device thruster display value should be zero. When the external force acts on the measuring device, the mobile part rotation axis produces micro-angle rotations; subsequently electromagnetic force balance is produced by the electromagnetic coil. Thus, the mobile parts very quickly return to the un-rotated status. At this time, the display will give the thrust measurement value. However, after the external force is removed, the flexible waveguide will produce an additional minute elastic force, meaning the reading on the voltage display will not be zero; this reading will be called the zero point. It is necessary to subtract this from the value of the thrust measurement value.

3 Thrust measurement actual results analysis

3.1 Experimental conditions

In the experiment a magnetron microwave source was utilized, with output power adjustable continuously within the range of 80 - 2500W. Output frequency is 2.45GHz.

The load can consume a thermal energy of 2500W.

3.2 Definition of measurement errors

In order to assess the accuracy of the experiment, four measurement errors are defined:

Calibration error

$$\eta_{\mathrm{c}} = \left| m_2 g/2 - (F_{\mathrm{cal}} - \varepsilon_0) \right| / (m_2 g/2) \times 100\%;$$

Thrust measurement system error

$$\eta_{\mathrm{s}} = \frac{\sum_{i=1}^{n_1} |\varepsilon_i|}{\sum_{i=1}^{n_1} \frac{1}{n_1} |F_{i,\mathrm{cal}} - \varepsilon_i|};$$

Repeatability error

$$\eta_{\mathrm{r}} = \max\left(F_1 - \sum_{\mathrm{i}=1}^{n_2} F_i/n_2, F_2 - \sum_{i=1}^{n_2} F_i/n_2, \cdots,\right.$$
$$\left. F_{\mathrm{n}_2} - \sum_{i=1}^{n_2} F_i/n_2\right) \Big/ \sum_{i=1}^{n_2} F_i/n;$$

Total error

$$\eta_{\mathrm{t}} = \eta_{\mathrm{c\,max}} + \eta_{\mathrm{s}} + \eta_{\mathrm{r}},$$

From which Fcal is the thrust display value under a standard weight, ε_0 is the zero point under the standard weight, n_1 is the number of calibrations, ε_1 is the ith calibration zero point, $F_{i,\,cal}$ is the thrust display value under the ith calibration, η2 is the number of experiments to measure thrust under propellantless microwave thruster normal working condition s, F_i is the thrust measurement experiment displayed thrust value, η is the total number of experiments.

3.3 Measurement results and analysis

Firstly, with microwave output power at 300-2500W, thrust measurement results show that the thrust direction is from the large end of the microwave cavity towards the small end. Figure 4 (a) shows the experimental measurements. The measurement results show that when microwave output power P = 300W, thrust reaches the first maximum value, approximately 310mN. Subsequently with an increase in power output, the thrust declines. When the output power is 800W, the thrust is minimized at 160mN. After the increase in output power, thrust increases, and with the maximum output power of 2500W, the maximum thrust reaches around 750mN. With the microwave output power at 80-1200W, the thrust measurement results show that the thrust direction is still from the large end of the microwave cavity towards the small end. Figure 4 (b) shows the experimental measurements. The measurement results show with the microwave output power at 300W, thrust reaches the first maximum value, approximately 270mN. Subsequently with an increase in power output, the thrust declines. When the output power is 600W, the thrust is minimized at around 180mN. After the increase in output power, thrust increases, when the output power is 1200W, the thrust is maximized at around 250mN.

When the microwave output power range is 300-2500W and 80-1200W, the thrust measurement direction and thrust size variation are consistent, showing that the experiment has good reproducibility. The only downside is that, when the thrust was at the lowest value, the microwave output powers were different. This may be caused by the instability of the output power of the microwave source. Reference [16] used classical electromagnetic theory to calculate the size and direction of propellantless microwave thruster theoretical thrust. The results are: The thrust direction is from the large end towards the small end. With other conditions fixed, thrust size is proportional to microwave output power. The theoretical calculations and experimental results for the direction of thrust were identical. However, the changes in thrust with variation in microwave power showed a large difference between theoretical results and experimental results. The

following analysis of the frustum microwave resonator actual resonance performance and microwave power output spectral characteristics analyzes this discrepancy.

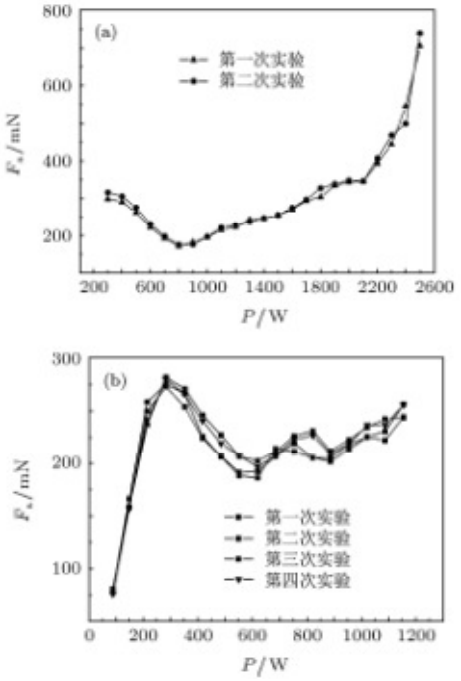

Figure 4 Different microwave output power range thrust measurement results (a) Output power ranging from 300-2500W; (b) output power range of 80-1200W

[LABELS: From top to bottom “First calibration”, “Second Calibration”, and on the second diagram “First calibration”, “Second calibration”, “Third calibration”, “Fourth calibration”]

A microwave network analyzer was used to measure this experiments’ frustum microwave resonator resonance curve, as shown in Figure 5. The vertical axis in Figure 5 represents the frustum microwave resonator return loss Lr = 10lg (Pr / Pi), wherein Pr is the reflected power from the cavity and Pi is the power of the input to the resonant cavity; the horizontal axis f is the output frequency. As the return loss is smaller, this shows that the cavity reflects less microwave energy, and absorbs more energy. When Lr = 0, the microwave power is totally reflected from the resonant cavity; when $Lr = Lr_{min}$, the resonator has reached a resonant state, the microwave power reflected from the resonator is minimum, and at this time, the frequency f0 is the resonant frequency. Frequency width is defined as $Lr = 0.707Lr_{min}$ with $\Delta f = f2-f1$ as the bandwidth of resonant frequency. Figure 5 gives the actual measured curve showing that the experimental frustum microwave resonator resonant frequency f0 = 2.450GHz, and the resonant frequency bandwidth $\Delta f = 0.0016$GHz. This shows that when the microwave radiation energy is distributed within the range of 2.4492-2.4508GHz, more than 90% of the microwave energy can be absorbed by the resonant cavity to produce net thrust.

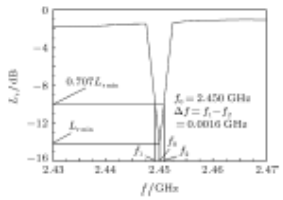

Figure 5 frustum microwave cavity actual resonance curve

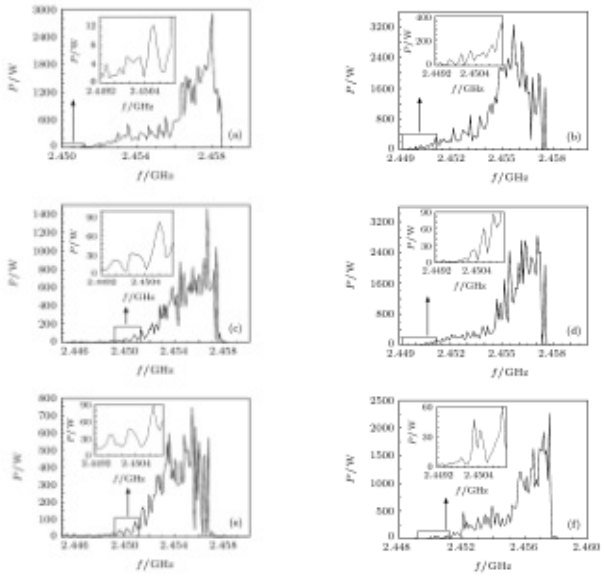

Figure 6 Magnetron microwave source spectral characteristics for different output powers, the inserts are a partially enlarged view of a selected frequency range (a) P = 200; (b) P = 300W; (c) P = 400W; (d) P = 500W; (e) P = 600W; (f) P = 700W

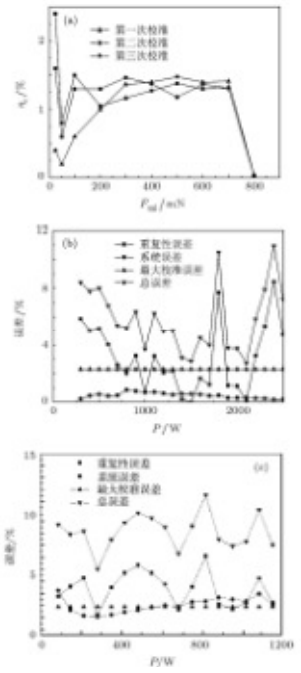

Figure 7 thrust measurement calibration error of experimental error (a); (b) 300-2500W power range measurement error; (c) 80-1200W power range measurement error;

[LABELS: a: The first calibration, The second calibration, The third calibration

B: Repeatability error, Systematic error, Maximum calibration error, Total error

C: Repeatability error, Systematic error, Maximum calibration error, Total error]

A frequency analyzer was used to measure the actual magnetron microwave source different output power P and output frequency f spectrum, as shown in Figure 6. Figure 6 shows the nominal output power of the microwave source at 200, 300, 400, 500, 600 and 700W, in the frustum microwave resonator the resonant frequency bandwidth range is 2.4492-2.4508GHz, the actual maximum output power of the microwave source was 13 120, 85, 65, 45 and 48W. Actual output power of the microwave source variation with output power is similar to that of thrust measurement changes. That is, actual output power is maximized at 300W output power. Thus, the thrust generated is also maximized; at 600W output power, the actual output power is minimized, thus, the thrust generated is also minimized; from which the actual output power of the microwave source variation with output power is similar to that of thrust measurement changes. This experiment shows that propellantless microwave thruster net thrust increases as microwave actual power increases, and this is consistent with the theoretical calculation results given in reference [16].

From the above error definitions and experimental data, the measurement error is determined as shown in Figure 7. The calibration curve shown in Figure 7 (a) shows that the maximum error is found in the minimum calibration thrust value at 2.4%. The minimum error is found in the maximum calibration thrust value, at 0.05%. The error curves displayed in Figure 7(b) and (c) show that at 300-2500W and 80-1200W output microwave power conditions, when the thrust maximum value is

750mN, the maximum measurement error is less than 12%; and in the maximum total error, the calibration error is 2.4%, the measuring system error is 3.5%, and repeatability error is 6.1%. This shows that the thrust measurement error comes mainly from the repeatability error; this is related to the stability of the propellantless microwave thruster microwave output power.

4 Conclusion

Indifferent equilibrium thrust measurement devices verify that, based on classical electromagnetic theory, creating a propellantless microwave propulsion system can produce a net thrust; Net thrust measurement of propellantless microwave thruster experimentation shows that the direction of net thrust produced by the propellantless microwave thruster is from the frustum microwave resonator big end to the small end. The results are consistent with theoretical calculations. When the magnetron microwave source output is 2.45GHz, with a microwave power of 300-2500W, the propulsion produced by the thruster is located in the range of 160-750mN, and the total measurement error is less than 12%. When the microwave source output is 2.45GHz, with a microwave power of 80-1200W, the propulsion produced by the thruster is located in the range of 180-270mN, and the total measurement error is less than 12%. Using a microwave network analyzer and spectrum analyzer for measurement, it was discovered that this experiment's frustum microwave resonator has an extremely narrow resonant frequency bandwidth, of only 0.0016GHz; furthermore, with the magnetron microwave source actual output power in this experiment, within this narrow frequency range, a non-linear change with the microwave output power is found. This leads to net thrust having a non-linear variation with microwave output power. However, spectrum data analysis shows that propellantless microwave thruster net thrust increases with microwave actual power. The results are consistent with theoretical calculations.

5 References

[1] Normile D 2010 *Science* 328 565

[2] Kuninaka H, Nishiyama K, Funaki I, Yamada T, Shimizu Y, Kawaguchi J 2007 *Propuls. Power* 23 544

[3] Kuninaka H, Nishiyama K, Funaki I, Shimizu Y, Yamada T, Kawaguchi J 2006 *IEEE Trans. Plasma Sci.* 34 2125

[4] Funaki I, Kuninaka H, Toki K 2004 *J. Propuls. Power* 20 718

[5] Kerr R A 1999 *Science* 285 993

[6] Anita S 2009 *J. Appl. Phys.* 105 093303

[7] Smirnov A, Raitses Y, Fisch N J 2007 *Phys. Plasma* 14 057106

[8] Yang J, Han X W, He H Q, Mao G W 2004 *J. Spacecraft Rockets* 41 126

[9] Yang J, Xu Y Q, Meng Z Q, Yang T L 2008 *Rev. Sci. Instrum.* 79 083503

[10] Yang J, Xu Y Q, Tang J L, Mao G W, Yang T L, Tan X Q 2008 *Phys. Plasma* 15 023503

[11] Johnson L, Young R M, Montgomery E E IV 2007 *AIP Conf. Proc.* 886 207

[12] Normile D 2010 *Science* 328 677

[13] Abdallah C T, Chahine E, Geogriev D, Schamiloglu E 2003 *AIP Conf. Proc.* 664 348

[14] Wang Y P 2007 *Engineering Electrodynamics* (Xi'an: Xidian University Press) p32 (in Chinese)

[15] Yang J, Yang L, Li P F 2011 *Acta Phys. Sin.* 60 124101